Rajesh Kumar

Nonlinear optical microscopy and Raman spectroscopy analysis of Osteoarthritis

Thesis for the degree of Philosophiae Doctor

Trondheim, May 2015

Norwegian University of Science and Technology
Faculty of Natural Sciences and Technology
Department of Physics

"In science there is only physics, all the rest is just stamp collecting." —
Lord Kelvin (1824-1907).

Abbreviations

OA	Osteoarthritis
ECM	Extra-cellular matrix
YLD	Years lived with disability
MRI	Magnetic resonance imaging
NLOM	Nonlinear optical microscopy
SHG	Second harmonic generation
p-SHG	Polarization second harmonic generation
ICRS	International cartilage repair society
OARSI	Osteoarthritis research society international
K/L	Kellgren-Lawrence
GAG	Glycosaminoglycan
SPGR	Spoiled Gradient Recalled
dGEMRIC	Gadolinium-Enhanced MRI of Cartilage
OCT	Optical coherence tomography
CT	Computed tomography
H & E	Hematoxylin and eosin
CLSM	Confocal laser scanning microscopy
NA	Numerical aperture
TPEF	Two-photon excited fluorescence
PSF	Point spread function
CW	Continuous wave
CCD	Charge coupled device
FE	Finite element
IR	Infra-red
UV	Ultraviolet

Acknowledgement

Rajesh Kumar   Trondheim, April 2015.

Table of contents

List of papers

- *Polarization second harmonic generation microscopy provides quantitative enhanced molecular specificity for tissue diagnostics.* **Rajesh Kumar**, Kirsten M. Grønhaug, Elisabeth I. Romijn, Andreas Finnøy, Catharina L. Davies, Jon O. Drogset and Magnus B. Lilledahl. *Journal of Biophotonics,* Wiley-VCH Verlag, Early view available online, DOI: 10.1002/jbio.201400086

- *Analysis of human knee osteoarthritic cartilage using polarization sensitive second harmonic generation microscopy.* **Rajesh Kumar**, Kirsten M. Grønhaug, Elisabeth I. Romijn, Jon O. Drogset, Magnus B. Lilledahl. *Proc. of SPIE- the international society for optical engineering.* Vol. 9129, 91292Z (2014). DOI: 10.1117/12.2051989.

- *Nonlinear optical microscopy of early stage (ICRS Grade-I) osteoarthritic human cartilage.* **Rajesh Kumar**, Kirsten M. Grønhaug, Catharina L. Davies, Jon O. Drogset, and Magnus B. Lilledahl. *Biomedical Optics Express* 2015, 6(5), 1895-1903. DOI: 10.1364/BOE.6.001895

- *Optical investigation of osteoarthritic human cartilage (ICRS Grade) by confocal Raman spectroscopy: A pilot study.* **Rajesh Kumar**, Kirsten M. Grønhaug, Nils K. Afseth, Vidar Isaksen, Catharina de Lange Davies, Jon O. Drogset and Magnus B. Lilledahl (Review).

- *Label free optical detection of ICRS grade in osteoarthritic chondrocytes by Raman microspectroscopy.* **Rajesh Kumar**, Gajendra P. Singh, Kirsten M. Grønhaug, Nils Afseth, Catharina L. Davies, Jon O. Drogset and Magnus B. Lilledahl. *International Journal of Molecular Sciences* 2015, 16(5), 9341-9353; DOI:10.3390/ijms16059341

Other publications

This section includes publications which do not fall under the subject of this thesis and is thus not included, but was completed during the Ph.D period as additional projects in collaborations.

- *Mueller matrix three-dimensional directional imaging of collagen fibers.* Pål G Ellingsen, Lars M Sandvik Aas, Vegard S Hagen, **Rajesh Kumar**, Magnus B Lilledahl, Morten Kildemo. *Journal of Biomedical Optics* 19(2), 026002 (2014). DOI: 10.1117/1.JBO.19.2.026002.

- *A facile and real-time spectroscopic method for biofluid analysis in point-of-care diagnostics.* **Rajesh Kumar**, Singh GP, Barman I, Dingari NC, Nabi G. *Bioanalysis,* a journal of future science group (fsg) 2013, 5(15):1853-61. DOI: 10.4155/bio.13.126.

- *Selective sampling using confocal Raman spectroscopy provides enhanced specificity for urinary bladder cancer diagnosis.* Barman I, Dingari NC, Singh GP, **Rajesh Kumar**, Lang S, Nabi G. *Analytical and Bioanalytical Chemistry* 2012, 404(10):3091-3099. DOI: 10.1007/s00216-012-6424-6.

ABSTRACT

Osteoarthritis (OA) is a highly prevalent, disabling, complex joint disorder, and a leading cause of individual and socioeconomic burden. The tissue that contributes the most extraordinary functional capacities and forms the bearing surface of all synovial (e.g., knee) joints, is articular cartilage. Degeneration of the articular cartilage is directly associated with the progression of OA. Due to the lack of resolution and sensitivity, currently used clinical imaging modalities (e.g., X-ray, MRI, and ultrasound) are not efficient in the assessment of early cartilage disorders. Nonlinear optical imaging and Raman spectroscopy are evolving, advanced microscopy and bio-analytical technique, respectively, which may be used for biomedical applications. Using such techniques in the analysis of different grades of osteoarthritic cartilage in humans rather than an animal model is more relevant to demonstrate the clinical potential.

The goal of this thesis is to demonstrate the capability of nonlinear optical microscopy (NLOM) and Raman spectroscopy for morphological and biochemical characterization of human articular cartilage obtained from the femoral condyle of the knee. Novel morphological features (like microsplits and wrinkles) in early stage of osteoarthritic cartilage were observed by second harmonic generation (SHG) microscopy; structures that would otherwise not be visible in existing clinical imaging modalities. Within the group of ICRS Grade-I cartilage, possibly distinct phases of OA were observed. In order to perform polarization-SHG (p-SHG) microscopy, a portable polarization optical module was developed and integrated in a commercial microscope. The presence of fibrocartilage in early stage (ICRS Grade-I) of OA was observed by p-SHG microscopy. Furthermore, it was demonstrated that alteration of the collagen molecule's pitch angle can be quantified by p-SHG microscopy. By using Raman spectroscopy, a relative assessment of proteoglycan and amide (ordered vs. disordered protein coil) content, in different grades of osteoarthritic cartilage (ICRS Grade-I, II, III), was performed and their respective indication was discussed. A correlation between two different clinical grading systems (ICRS Vs. OARSI) of OA was evaluated. Additionally, a label free analysis of chondrocytes isolated from osteoarthritic cartilage was performed, which demonstrated that Raman micro-spectroscopy may reveal changes in biochemical compositions at the cellular level. The bio-mechanical characterizations of osteoarthritic articular cartilage are in progress. As a future plan, the correlations between novel morphological, bio-chemical and biomechanical features will be

investigated. Such correlations may enhance our understanding about the progression of OA.

NLOM and Raman spectroscopy are minimally invasive and label free techniques. By the use of a miniaturized fiber based probe head, these techniques can be integrated with modern clinical arthroscopes and thus potentially be used for *in vivo* analysis. Our proof-of-concept study encourages further investigation for the development of NLOM and Raman arthroscope as a potential diagnostic tool for the use in Orthopaedics.

INTRODUCTION AND BACKGROUND

(a) Osteoarthritis

Osteoarthritis (OA) is a complex musculoskeletal disorder whose origin is not exactly clear. The views about OA are continuously evolving. It is believed that the disease primarily affects the quality of articular cartilage, both collagen and other extra-cellular matrix (ECM) components, as well as the underlying bone. It is a leading cause of disability among older adults. In Europe, a total joint replacement surgery is being done due to OA every 1.5 minutes. In the United States, situation is even worse, where a total of 500,000 replacement are performed every year[1-3]. It is a major public health issue of increasing individual and socioeconomic burden. It was Recently found that it is the fastest increasing major health condition in terms of global 'years lived with disability (YLD)' ranking[4]. It results in extensive use of medical, physical and surgical therapy and therefore has major socioeconomic implications.

Although the gross morphological changes in arthritis are known, relatively little is known about the underlying mechanism associated with the progression of OA. The inherent heterogeneity and slow evolution of the joint disorder, amplified by a lack of accurate characterization methods, complicate early diagnosis. In fact, there is no "gold standard" available which can provide a clear dichotomy between those with and without the disorder. However, varieties of diagnostic criteria are under development. Currently a combination of clinical symptoms and test are being used to diagnose OA.

(b) Clinical features of Osteoarthritis

Pain in the joints, stiffening of the joints after inactivity or during wakeup time in morning, restricted movement of the joint, bony swelling, crepitus and deformities of the joints are known clinical features associated with OA. However, some of these depend on the general health of the patient and lack reproducibility, which creates difficulty in defining OA clinically. Moreover, several features are also present in other form of arthritis. Blood tests e.g., erythrocyte sedimentation rate and/or urine test helps in distinguishing OA from other inflammatory forms of joint disorder. After the identification of clinical symptoms, in order to verify OA, the clinician can choose other diagnostic criteria based on radiographic or other sophisticated imaging modalities changes.

(C) An overview of clinical imaging modalities in the context of OA

- **Radiography**

The general pathologic definition of OA emphasizes the progressive thinning of articular cartilage and bone remodeling. Conventional radiography is a straightforward and least expensive way for imaging the joint. Although, cartilage cannot be visualized directly in radiography, the technique provides an indirect way to determine the thickness of cartilage, marginal osteophytes and meniscal integrity. This method of OA assessment relies mainly on lesions associated with subchondral bone and narrowing of joint space. A continuous increase in joint space narrowing indicates progression of OA. Depending on the joint space narrowing, a score called Kellgren-Lawrence (K/L) score is assigned[5]. K/L score is a widely accepted method for the evaluation of the severity of OA. Figure 1 shows the X-ray data from patients with OA (grades 1 - 4) and acute inflammatory conditions of the knee joints[6].

Figure 1: X-ray image of patients with osteoarthritis[6] (reproduced with kind permission). Classification of grade is based on K/L score.

Assessment of OA by radiography has a few issues. First, it lacks sensitivity. Second, it emphasizes only bone changes and bone abnormalities. Due to these reasons joint damage appears on plain radiograph only at advanced stage of OA. Moreover, K/L score is very subjective and has poor reproducibility[7]. The correlation between radiological diagnosis and visual gross assessment (depth and size of cartilage lesion) of OA severities is not very encouraging[8]. Therefore, the prediction of cartilage condition by radiographic assessment of joint space is considered to be inaccurate[8,9]. Several investigators have worked to reduce the inter- and intra-reader variability and tried to enhance the reliability[10,11]. Protocols for standardization of radiographic assessments are in progress[7,12]. However recently the

Osteoarthritis Research Society International (OARSI) working group still recommended the option of radiographic joint space width for clinical trials of structure modification[13] provided radiographic image were obtained with the knee in a standardized flexed position[14]. It is worth to note that the measurement of joint space width by radiology is actually associated with several pathologies involved in OA including damage of articular cartilage. Therefore, in order to directly image and asses the morphology of cartilage -MRI, is becoming increasingly important[15].

- **Magnetic Resonance Imaging (MRI)**

MRI is not often used in routine clinical assessment or diagnosis of OA. In comparison with radiography, it is more suitable for the study of cartilage disease progression and treatment response in OA. It offers multiplanar cross sections and better image resolution than radiography, without ionizing radiation. It is capable of imaging all soft tissue components of a joint simultaneously and is therefore an important imaging modality in the context of whole organ imaging (e.g., full knee joint). By utilizing this modality, in a knee joint it is possible to obtain information about articular cartilage[16,17], ligaments[18], tendons[18], and bone lesions[19,20]. Morphological assessment provides information about the structural integrity, thickness and loss of cartilage. Currently for the morphological imaging of cartilage three-dimensional spoiled gradient recalled echo imaging with fat suppression (3D-SPGR) technique is in use[21,22]. This sequence creates contrast in the image by acquisition of high signal from cartilage and low signal from adjacent joint fluid.

Besides morphological assessment, recently, MRI is also evolving to provide physiological content of cartilage including information about the status of glycosaminoglycan (GAG) and collagen matrices. T1rho imaging is a promising method which may be sensitive to early proteoglycan depletion[23] and hence may be effective in visualizing early stage OA[24,25]. During progression of OA the physiochemical interactions in the macro-molecular environment are disrupted due to proteoglycan depletion and therefore T1rho can be used to measure the interaction between ECM environment and motion-restricted water molecules[26].

Atoms having odd number of proton/neutrons possess net nuclear spin and therefore exhibit the phenomena magnetic resonance. The nuclei of Sodium-23(Na^{23}) in addition to hydrogen (^1H) are useful for cartilage imaging. MRI imaging technique indirectly utilizes the negative fixed charge density in ECM of cartilage. This negative charge arises due to presence of GAG chains and carboxylate groups in the cartilage matrix. Due to damage in

cartilage, proteoglycan depletion (i.e., change in concentration of negatively charge ions) occurs and therefore Na^{23} signals decline[27,28]. This technique has shown promising results and may be useful in depicting the proteoglycan depletion region[29] in articular cartilage. However, this technique needs special coils (transmit and receive) and more imaging acquisition time to achieve good contrast (high signal to noise ratio).

To improve visibility, Gadolinium based contrast agents are commonly used in MRI. It works similarly to Na^{23} imaging and accumulation depends on the distribution of negative charge density in the cartilage matrix. After the injection it penetrates the cartilage and relatively accumulates more where the GAG content is less. Subsequent T1 imaging or imaging with 3D-Spoiled Gradient Recalled (SPGR) pulse sequences provides an image with a depiction of relative GAG distribution. In general this method is referred to as Delayed Gadolinium-Enhanced MRI of Cartilage (dGEMRIC), where the term delay corresponds to the time required for the Gadolinium ion to penetrate the cartilage[30,31]. However this technique is also time consuming and is difficult to perform on a routine basis.

- **Ultrasound**

Cartilage can be identified by ultrasound and is sensitive to its physical properties[32]. However, in clinical practice visualization of cartilage *in vivo* in the central load bearing areas of a joint is difficult, and therefore the clinical relevance to articular cartilage is questionable. The interface between soft tissue and bony cortex is highly reflective and therefore prevents the sound wave to penetrate the cortex. Hence it prevents the visualization of pathological changes inside the bone. Therefore, in contrast to MRI, subchondral bone changes (e.g., bone marrow lesions) are not readily apparent in ultrasound imaging. The main advantage of ultrasound over radiography is the detection of synovial pathologies including hypertrophy, vascularity, and presence of synovial fluid[33,34]. These conditions are more relevant to rheumatoid arthritis. It is proposed that besides rheumatoid arthritis it may also be applied to OA because the difference in synovial inflammation between the two diseases is quantitative[34,35]. The application and utilization of ultrasound for OA, the large scale investigation is on the way[36]. The operator dependency and lack of resolution are major limitations associated with ultrasound imaging.

- **Arthroscopy and Optical Coherence Tomography**

Arthroscopy is the another standard clinical option for assessment of cartilage or for evaluating chondrosis and pre-OA chondral lesions that do not involve bone and are not visible on radiographs[37], but this method of assessment is subjective. Optical Coherence Tomography (OCT) is an emerging novel optical imaging technique that provide cross-sectional images and quantitative information[37] about the disease state of articular cartilage. This technique is the optical analog of ultrasound and is capable of providing a high-resolution ($\sim$ 10 µm) digital images. A representative arthroscopically firm and arthroscopic fissuring cartilage and corresponding OCT image is shown in figure 2. Although OCT provides reasonably better resolution than other clinical imaging tool for morphological assessment of cartilage, it lacks specificity, requires image post-processing and assessment is operator dependent[38].
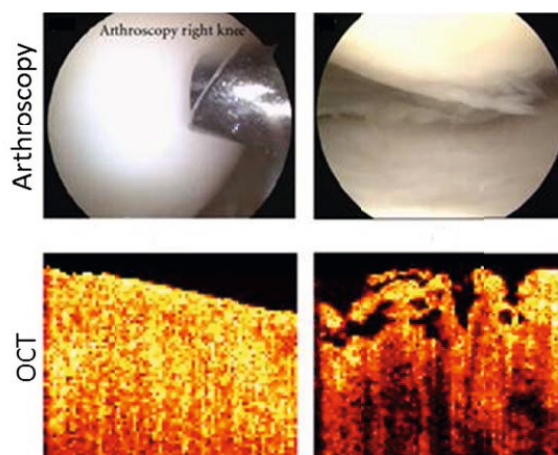
Figure 2: A typical arthroscopy and OCT image obtained from a firm and fissuring cartilage[39](reproduced with kind permission).

Table-I: A comparison of different imaging modalities

Imaging modality	Imaging depth	Resolution
Confocal microscopy	~ 0.2 mm	~ 1 µm
Two photon microscopy	~ 0.5 mm	~ 1 µm
Optical coherence tomography	~ 1-2 mm	~ 10 µm
Ultrasound	~ 60 mm	~ 150 µm
High resolution CT	Whole joint	~ 300 µm
MRI	Whole joint	~ 1 mm

- **Histopathology**

As mentioned, OA is a complex disorder which primarily affects the quality of articular cartilage and underlying bone. Hyaline cartilage is mostly found in diarthroidal joints. It covers the head section of the joint bone, typically called articular cartilage. Cells found in the articular cartilage are called chondrocytes. They are distributed in a circumscribed space called the lacunae. These cells form 1-5% of the tissue volume. The main function of the chondrocyte is to produce large amounts of ECM which mainly comprise collagen (60% of dry weight), proteoglycans (25–35% of dry weight), and non-collagenous proteins (15–20% of dry weight)[40]. Water forms the 65-80% of the cartilage and plays an important role in nutrient transfer and load distribution. In hyaline cartilage collagen molecules are mainly type II with smaller amounts of type IX and XI collagens. Collagen molecules provide tensile strength while proteoglycan molecules provide compressive resistance to the articular cartilage.
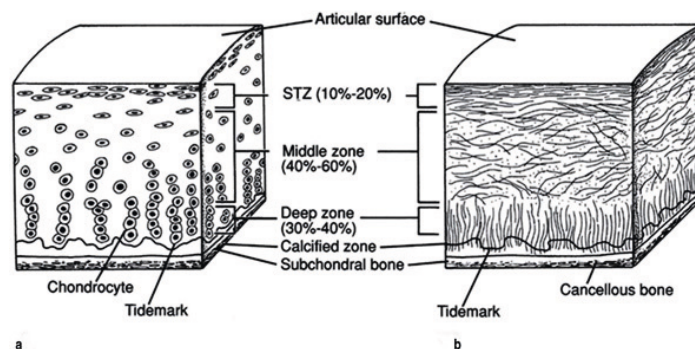
Figure 3: A schematic diagram that represents different zones of articular
cartilage[41](reproduced with kind permission).

Articular cartilage is mainly composed of three zones (superficial, middle and deep). A
schematic diagram that represents different zones of articular cartilage is shown in figure 3.
The transition among these zones is somewhat continuous but the calcified cartilage is
separated by a distinct mark of mineralization called the tidemark. In the superficial zone
chondrocytes and collagen fibers at the surface of the cartilage are mostly aligned parallel
to the surface and contribute to resisting shear stress. In the middle zone, the chondrocytes
and collagen fibers are more randomly aligned to distribute the load throughout the tissue
and, in the deep zone aligned perpendicular to the surface and thus plays an important role
in securing the cartilage to the bone by anchoring the collagen fibrils to the subchondral
bone[41,42].
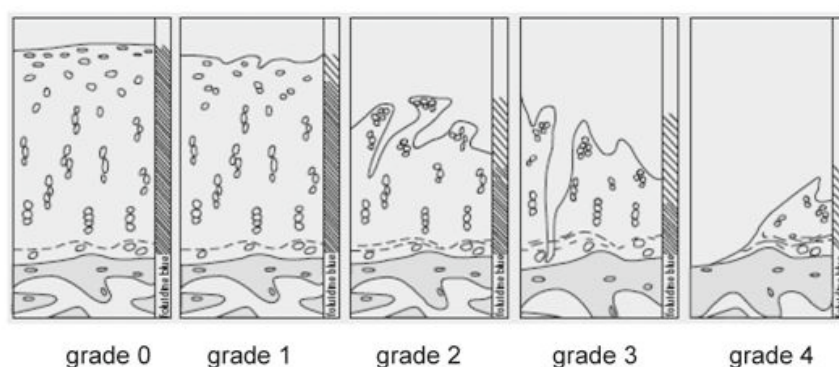
Figure 4: Histological evaluation (Otte's Method[43]) of cartilage degradation in
OA[44](reproduced with kind permission).

Cartilage histopathologic features provide characteristics associated with biological activities and progression of OA. Histological grading and staging of OA in a standardized format play an important role for the international community in order to compare different studies. Several grading system have been adopted for characterization of cartilage. Currently, histopathological assessment of cartilage are mainly based on Collins scale[45,46], Otte's method[43], Mankin score[47] and OARSI grade[48]. Osteoarthritic grade is defined by depth progression into cartilage and serves like an index for severity of the disease. A schematic diagram (figure 4) shows the typical morphology of articular cartilage and respective assignment of osteoarthritic grade during the progression of OA[43]. The prominent histological changes associated with cartilage in OA are erosion, fibrillation, clefts, chondromalacia, loss of metachromasia, duplication of tidemark and cloning of chondrocytes[49-51]. Typically hematoxylin and eosin (H & E) histology is sufficient to interpret the pathology of cartilage. However, some special histochemical stains like alcian blues and safranin-O (cationic dyes) may be used to assess the presence of proteoglycan in cartilage. Based on the mentioned structural/morphological features and stains, the grade of OA is defined in histological sections which are generally assessed at low power magnification. However, in histological grading system the interrelation between the assessment variables is not linear and wide interobserver variations were found for mild or earlier phases of the disease in many OA model systems[48]. The reproducibility and the validity of the grading system for osteoarthritic cartilage has been questioned formally[52,53].

(d) Role of nonlinear optical microscopy in the investigation of OA

Degradation of articular cartilage is directly associated with progression of OA. Radiographic imaging cannot provide direct information of degradation and morphology of cartilage. Morphological changes in cartilage at the micron level and structural change associated with collagen fibers are difficult to investigate with MRI and ultrasound due to lack of resolution. Although OCT provides reasonably good resolution ($\sim$ 10μm), it lacks the specificity to distinguish the biological constituents. Arthroscopy remains a useful minimally invasive technique but it also lacks high resolution and specificity. Nonlinear optical microscopy (NLOM) is a useful technique to provide high resolution ($\sim$ 1 μm) images of intact tissue (table-I) without any need of sectioning and staining of cartilage. It utilizes endogenous optical signals from the ECM and chondrocytes which allow an improved way of investigation for chondrocytes and matrix physiology with minimal artifacts. It provides better cell

viability, less photo-degradation and improved depth penetration compared to confocal laser scanning microscopy (CLSM)[54,55].

Collagen is one of the major constituents of the cartilage matrix. Highly noncentrosymmetric molecular assemblies of fibrillar collagen make it an extremely bright second-harmonic generator. As a result, second harmonic generation (SHG) microscopy has recently become a robust tool for imaging tissue structure with cellular resolution[56-58]. SHG microscopy has a high molecular specificity for collagen fibers. Therefore, it can be used to characterize early structural and/or morphological modifications in the collagen network inside cartilage matrix during progression of OA. Moreover, by utilization of polarization second harmonic generation (p-SHG) microscopy, it is also possible to identify the molecular sources of SHG scatters (e.g. different types of collagen fibers) based on their susceptibility (χ) value as a quantitative parameter[59,60], again without resorting to external labeling agents. By using intrinsic auto-fluorescence, another nonlinear optical imaging modality called two-photon excited fluorescence (TPEF) microscopy can also provide the morphology of ECM of cartilage and can characterize chondrocytes in the lacuna. Figure 5(a) is a typical SHG image that shows the distribution of collagen fibers on the surface of the articular cartilage (superficial region), while, figure 5 (b) represents a combination of SHG and TPEF images that show the distribution of chondrocytes (green) within the collagen (red) network in the deep zone of articular cartilage obtained from a chicken knee. Red and green are false color and as mentioned earlier, signals were originating from endogenous molecules.
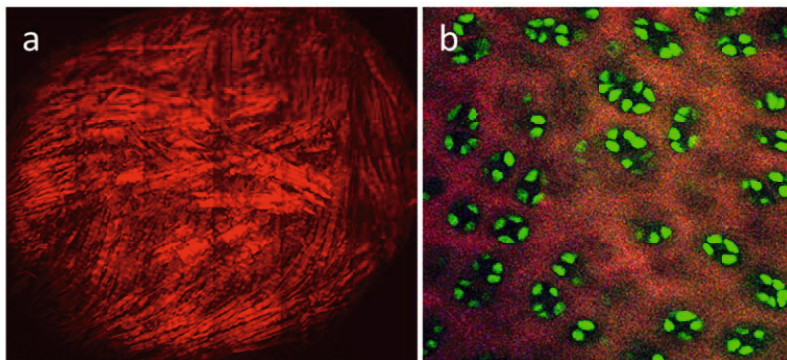
Figure 5: (a) SHG image shows the collagen network in the superficial region of the articular cartilage (size: 1350 μm × 1125 μm). (b) A combination of SHG (red) and TPEF (green) images show the distribution of chondrocytes within the collagen network in the deep zone of the articular cartilage (size: 225 μm × 225 μm).

Inherent 3-D optical sectioning capability of NLOM enables the technique to provide depth-dependent changes in tissue morphology and composition. Using backscattered experimental geometry, NLOM technique is not limited by sample thickness. This demonstrates that the technique is compatible with *in vivo* investigation by the use of an endoscopic probe, which necessarily uses the backscattered signal. Miniaturized multiphoton probes for endoscopic applications have been demonstrated by several groups[61,62]. Structural and morphological characterization of the cartilage matrix at micron level resolution with high specificity and sensitivity potentially *in vivo* is not possible by other clinical imaging modalities. Therefore, investigation of osteoarthritic cartilage by NLOM may reveal hidden features of OA. It can help in understanding the mechanism of disease and ultimately may provide a biomarker for early diagnosis of OA.

(e) Role of Raman spectroscopy in the investigation of OA

While the "wear and tear" model of OA is becoming old fashion, the molecular /enzymatic role in progression of OA is becoming more relevant in modern investigations. Characterization of molecular and biochemical changes that differentiate advanced diseased early stages or normal tissue is a major area of current research in OA. Currently used clinical imaging modalities (e.g. CT, MRI) provide unique and often complementary information to the rheumatologist but they fail to provide crucial information about the biochemical composition of the components of ECM at the molecular level. Changes at molecular level occur before macroscopic changes[63,64]. This information can help in understanding the underlying pathogenic mechanism associated with progression of OA. Moreover, a technique which can detect changes at the molecular level in early stage of the disease may play a crucial role in early stage diagnosis of a joint disorder.

The Light based vibrational spectroscopic technique-Raman spectroscopy can be used to obtain information about the composition and the chemical environment of the constituents of a tissue. It provides information at the molecular level potentially *in-vivo* (by the use of a miniaturized probe), without any external labelling and preparation of tissue samples[65]. Moreover, Raman microspectroscopy can provide information at a submicron spatial resolution[66].

Investigation of osteoarthritic cartilage

During the last decade, Raman spectroscopy has been employed for studying ECM of musculoskeletal tissues. However, most of the investigations of musculoskeletal tissues are focused on the analysis of bone tissue[64,67-72]. Because the underlying bone is exposed only during the most advanced stage of osteoarthritis (i.e., ICRS Grade IV), to detect early-stage osteoarthritis *in vivo*, it is necessary to perform Raman analysis on the articular cartilage rather than on the bone.

Over the past few years, several groups have used Raman spectroscopy to analyze the properties of cartilage. However, most studies have focused on the assignment and the structure of Raman bands [64,73] rather than investigation of the disease. Although a few reports are available on induced OA[74] and detection of proteoglycan[75] in animal model, investigation of human rather than animal cartilage is potentially more relevant to clinical application.

Investigation of osteoarthritic chondrocytes

The balance between anabolic and catabolic processes (homeostasis) determines the integrity of articular joint tissue. The structural breakdown of collagen and proteoglycans in the ECM of cartilage during progression of OA is believed due to an imbalance in homeostasis because of increased catabolic activity by chondrocytes[76]. Several studies also show that progression of OA is associated with increased chondrocyte cell death.[49] Investigations at the cellular level are, therefore, important in understanding the progression of OA as well as other musculoskeletal disorders.

Raman micro-spectroscopy has numerous times successfully demonstrated early detection of neoplasia[77], differentiation of tumors grades[78], and been useful in providing sub-cellular information from living cells[79,80]. Therefore, label free investigation of chondrocytes isolated from different grade of osteoarthritic cartilage by Raman microspectroscopy may explore molecular features associated with progression of disease at the cellular level.

THEORETICAL

- **Second harmonic generation (SHG) microscopy**

Second harmonic generation (SHG) is a nonlinear optical process that was discovered in 1961 by Frankel et al[81]. The process of SHG is shown in a schematic diagram (figure 6). An incoming laser beam at frequency ω enters into a nonlinear optical material and a nonlinear (two-photon) optical effect occurs (figure 6a) in which two photons combine together and generate a new photon at frequency 2ω. The energy level scheme of SHG process, also called frequency doubling, is shown in figure 6b. Under proper circumstances, the efficiency of the process can be more than 50%[82].
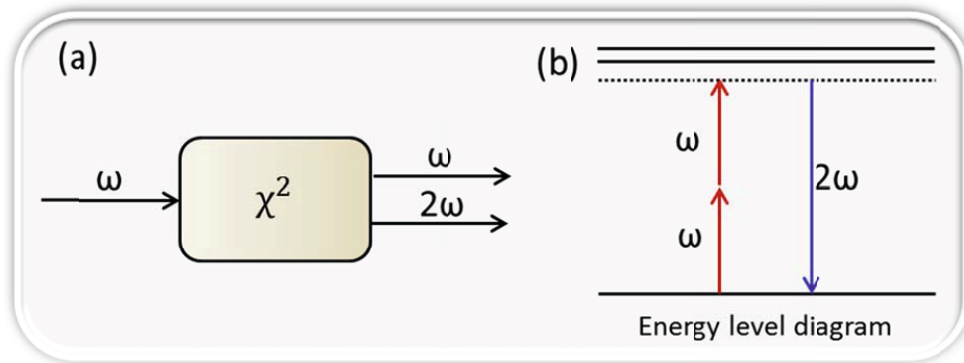
Figure 6: Second harmonic generation process

The response of dielectric material to the incident oscillating electric field (E) can be described in matrix form as follows:

$$P_i = \varepsilon_o \left(\sum_j \chi_{ij}^{(1)} E_j + \sum_{jk} \chi_{ijk}^{(2)} E_j E_k + \sum_{jkl} \chi_{ijkl}^{(3)} E_j E_k E_l + \cdots \right)$$

Where P_i is the induced polarization and $\chi^{(n)}$ is the nth order susceptibility of the material. For low field intensities, the polarization of a material depends to a good approximation only on the linear susceptibility $\chi^{(1)}$ of the matter and linearly on the incident electric field. For more intense fields, higher order susceptibilities (n>1 i.e. 2, 3…) play an important role. SHG is governed by second order nonlinear susceptibility coefficient $\chi^{(2)}$ which is a third-rank tensor and has 27 components. Considering cylindrical symmetry for collagen fiber, only four

independent χ-tensor elements are left[83]. By performing excitation polarization measurements, these independent χ-tensor components can be used for pathological characterization of connective tissues including articular cartilage[59,60,84]. The value of tensor $\chi^{(n)}$ decreases rapidly with increment in 'n', which indicates that higher order nonlinear process are very weak responses to the driving optical wave. The prediction of SHG can be performed by calculation of wave propagation. The equation of propagating wave can be written as follows:

$$\nabla^2 \widetilde{E} - \frac{n^2}{c^2} \frac{\partial^2 \widetilde{E}}{\partial \widetilde{p}^{NL} t^2} = \mu_0 \frac{\partial^2 \widetilde{p}^{NL}}{\partial t^2}$$

Where n, c, $\widetilde{p}^{NL}$ and μ_0 denotes the refractive index of the material, the speed of light, and the nonlinear contribution to the polarization and magnetic permeability of free space, respectively. Considering incident fundamental and emitted SHG wave to be plane waves of the form:

$$\widetilde{E}_j(z,t) = E_j(z) \, e^{i(k_j z - \omega_j t)} + cc$$

Where j=1,2 and $\omega_1 = \omega$ and $\omega_2 = 2\omega$. $E_j(z)$ is the spatial field amplitude of the field j and cc is the complex conjugate. The nonlinear component of the polarization can be written as

$$\widetilde{P}_2(z,t) = P_2(z) \, e^{i(2k_1 z - 2\omega t)} + cc$$

Where the complex amplitude of nonlinear polarization can be written as $P_2 = \varepsilon_0 \, \chi^{(2)} E_1^2$. Now, the equation of propagating wave can be re-written as follows

$$\frac{d^2 E_2}{dz^2} + 2ik_2 \frac{dE_2}{dz} - k_2^2 E_2 - \frac{(2\omega)^2 n_2^2}{c^2} E_2 = -(2\omega)^2 \, \varepsilon_0 \mu_0 \chi^{(2)} E_1^2 e^{iz(2k_1 - k_2)}$$

By applying slowly varying amplitude approximation the above equation can be simplified. Therefore, the first term can be neglected as it is very small with respect to second term. Remaining third and fourth term is cancelled out and simplified form of the equation can be written as follows

$$\frac{dE_2}{dz} = \frac{2i\omega}{n_2 c} \, \chi^{(2)} E_1^2 e^{iz(2k_1 - k_2)}$$

Now the simplest solution of this equation can be obtained under the low depletion approximation i.e. conversion of second harmonic is so small that the fundamental field (E_1) remains essentially almost constant. Considering E_1 as constant and solving the equation by direct integration for a propagation distance L, the amplitude of SHG field (E_2) can be written as

$$E_2(L) = \frac{2i\omega}{n_2 c} \chi^{(2)} E_1^2 \frac{e^{i\Delta k} - 1}{i\Delta k L}$$

Where $\Delta k = 2k_1 - k_2$. As we know that the relation between intensity and field strength is $I = 2n\left(\frac{\epsilon_0}{\mu_0}\right)^{1/2} |E^2|$. Therefore, the intensity of SHG radiation (I_2) can be written as

$$I_2(L) = \left(\frac{\epsilon_0}{\mu_0}\right)^{1/2} \frac{2\omega^2 \left\{\chi^{(2)}\right\}^2 I_1^2 L^2}{n_1^2 c^2 n_2} \left\{ \sin c^2 \left(\frac{\Delta k L}{2}\right) \right\}$$

The equation represents that when phase matching condition is satisfied (i.e. $\Delta k = 0$), the last term becomes unity and therefore the SHG intensity (I_2) increases as the square of the interaction length (L) as well as incident excitation intensity (I_1)[85,86] However, for the case of biological tissues, perfect phase matching is never achieved. Moreover, the molecules (e.g., collagen) are not perfectly aligned in a tissue. Thus, a strict phase matching requirement in tissue is relaxed and nonzero Δk is allowed, in such a way that the SHG signal vary in a sinusoidal way with coherence length (L). A general model for phase matching condition was developed which show that smaller and larger value of Δk are associated with primarily forward and backward SHG, respectively[87].

- **Two-Photon Excitation Fluorescence (TPEF) microscopy**

The theory of Two-photon excitation was first predicted by Maria Goeppert-Mayer in 1931[88] and first experimentally was observed by Wolfgang Kaiser in 1961[89]. The concept of two-photon excitation is based on the idea that two photons of comparably lower energy than needed for one photon excitation can also excite a fluorophore in one quantum event. Each photon carries approximately half the energy necessary to excite the fluorophore and arrives within a time window of an attosecond (10^{-18} s) and combined together to excite the molecule as a single quantum event (figure 7a). However, in principle, any combination of photons of different energies that sum up to provide an equivalent energy difference is possible.
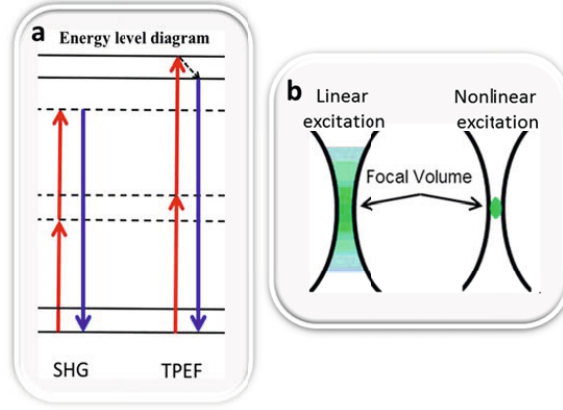
Figure 7: (a) Energy level diagram of SHG and TPEF process. (b) A schematic diagram that compares the linear and nonlinear excitation focal volume.

In nonlinear optical phenomena including TPEF microscopy, a high numerical aperture microscope objective is required to focus a diffraction limited spot in the excitation material. The spatial profile of the beam in the focal plane for a focusing beam of wavelength λ and a circular lens of NA= sinα, is given by[90,91]

$$I(u,v) = \left| 2 \int_0^1 J_0(v\rho) e^{-\frac{1}{2}u\rho^2} \rho d\rho \right|^2$$

Where J_0 is a zeroth order Bessel function, $u = 4k\,sin^2(\alpha/2)z$ and $v = k\,sin(\alpha)r$ are the arial and radial co-ordinates respectively normalized to the wave number $k = 2\pi/\lambda$. Since TPE process is proportional to the square of the incident photon flux, the point spread function (PSF) is given by $I^2(u/2,\,v/2)$. In comparison with 1P-PSF, $I(u,v)$, the TPE process has several differences that provide distinct advantages over confocal detection in biomedical imaging applications. In case of TPEF, photodamage and photobleaching are limited only to the focal point and do not occur above or below the focus (figure 7b). Other important advantages include deeper penetration depth in the tissue and higher light collection efficiency.

It has been shown that the number of photons absorbed per fluorophore per pulse, n_α, is given by[92]

$$n_\alpha = \frac{p_0^2 \delta}{\tau_p r_p^2} \left(\frac{(NA)^2}{2\hbar\lambda c} \right)^2$$

Where p_0 is average laser intensity, δ is fluorophore's two photon absorption at wavelength λ , τ_p is the pulse duration, r_p is pulse repetition rate, $\hbar$ is Planck's constant, c is speed of light and NA is numerical aperture of microscope objective. This equation shows that if we keep the average power and repetition frequency of the laser constant, the probability of excitation can be increased by decreasing the pulse width (e.g., from pico-second to femto-second pulse) of the laser and increasing the NA of focusing objective. Increasing the NA represents confinement of the excitation laser power to a smaller focal volume, and thus, enhancing the probability of two photon quantum mechanical event.

In TPEF microscopy, most commonly, a femto-second laser is used. However, as shown in above equation, pico-second laser can also be used but with less efficiency. Continuous wave laser excitation source was also demonstrated for TPEF microscopy[93]. The main motivation to use CW laser over femto/pico second laser is to show the reduction in system cost. However, a CW light source (ArKr laser) requires a ~200 fold increase of average power to achieve the same excitation rate as obtained with a femto-second laser**.**

- **Raman spectroscopy**

The phenomena of light scattering had long been studied by Rayleigh (1871), Einstein (1910) and others, but no change of wavelength was observed. Scattering in the X-ray region by Compton (1923) showed the idea of inelastic scattering. Then, a new kind of secondary radiation (induced radiation from atoms and molecules) was reported from Kolkata (India) by Raman and Krishnan (1928), later termed as the 'Raman effect'.

In Raman spectroscopy, the sample is irradiated by an intense laser beam (v) and the scattered light is detected on charge coupled device (CCD) array. The scatterd light are of two types. First, Rayleigh scattering (v) which is strong sccatering and of the same frequecy as the excitation laser (v). Second, Raman scattering which is a very weak scattering (10^{-7} of incident photons) and has frequency $v - v_f$ (Stoke's Raman) and $v + v_f$ (Anti-Stoke's Raman), where v_f is the vibrational shift (figure 8). Therefore, in Raman spectroscopy we measure the vibrational frequencies of the molecule as a shift from incident frequency in the form of a spectrum. In contrast to Infra red (IR) spectra where absorption of IR light by the sample as a function of frequency is measured, Raman spectra are measured in UV-Visible region as well. Moreover, Raman spectroscopy requires minimal sample processing with respect to IR spectroscopy and can be performed in physiological environment and is therefore highly suitable for biomedical applications.
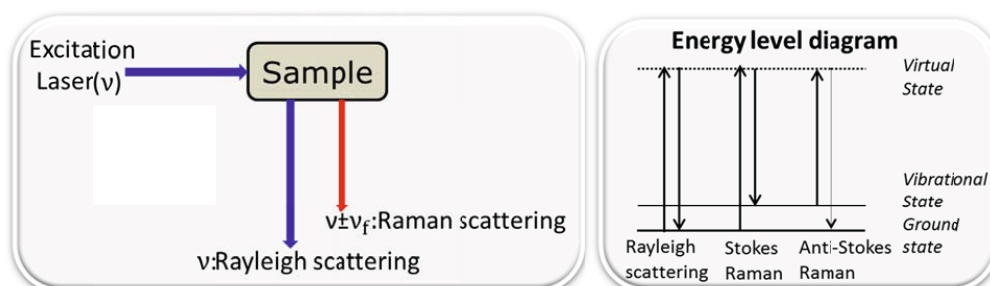
Figure 8: The different possibilities of light scattering: Rayleigh scattering, Stokes Raman scattering and anti-Stokes Raman scattering.

The fluctuation of the electric field strength in a laser beam with time can be written as

$E = E_0 \cos(2\pi v t)$

Where E_0 is the amplitude and v is the frequency of laser beam. If a diatomic molecule is excited by the laser beam then the dipole moment can be expressed as

$P = \alpha E = \alpha E_0 \cos(2\pi v t)$

Where α is a propotionality constant and is called polarizability. If the vibrational frequency of the molecule is v_f, the nuclear displacement (Δr) can be written as

$\Delta r = r_0 \cos(2\pi v_f t)$

Where r_0 is the amplitude of vibration. For a small amplitude of vibration, the instanteneous polarizability at some distance, r_0, away from the molecule's equilibrium geometry can be written as

$\alpha = \alpha_0 + \left(\dfrac{\partial \alpha}{\partial r}\right)_0 \Delta r$

Where α_0 is the polarizability at molecule's equilibrium geometry. Now by putting the value of α, P can be rewritten as follows

$P = \left\{\alpha_0 + \left(\dfrac{\partial \alpha}{\partial r}\right)_0 \Delta r\right\} \{E_0 \cos(2\pi v t)\}$

$P = \alpha_0 E_0 \cos(2\pi v t) + \left\{\left(\dfrac{\partial \alpha}{\partial r}\right)_0 \Delta r\right\} \{E_0 \cos(2\pi v t)\}$

$P = \alpha_0 E_0 \cos(2\pi v t) + \left\{\left(\dfrac{\partial \alpha}{\partial r}\right)_0 r_0 \cos(2\pi v_f t)\right\} \{E_0 \cos(2\pi v t)\}$

$$P = \alpha_0 E_0 \cos(2\pi v t) + \left(\frac{\partial\alpha}{\partial r}\right)_0 r_0 E_0 \cos(2\pi v_f t)\cos(2\pi v t)$$

$$P = \alpha_0 E_0 \cos(2\pi v t) + \frac{1}{2}\left(\frac{\partial\alpha}{\partial r}\right)_0 r_0 E_0\, 2\cos(2\pi v t)\cos(2\pi v_f t)$$

$$P = \alpha_0 E_0 \cos(2\pi v t) + \frac{1}{2}\left(\frac{\partial\alpha}{\partial r}\right)_0 r_0 E_0\, [\cos\{2\pi\,(v + v_f)t\} + \cos\{2\pi\,(v - v_f)t\}]$$

First term repersents the light of frequencey $'v'$, which repersents the Rayleigh scttering, while second term repersents Raman scattering of the frequency $'v + v_f'$ (anti-Stoke's) and $'v - v_f'$ (Stoke's). This equation also illustrates that if the rate of change of the polarizability is zero i.e., $\left(\frac{\partial\alpha}{\partial r}\right)_0 = 0$, the molecule is not Raman active.

DISCUSSION

- **Summary of the papers**

Paper-1: *Polarization second harmonic generation microscopy provides quantitative enhanced molecular specificity for tissue diagnostics.*

The susceptibility (χ) tensor element ratio can be used to quantitatively identify the different types of SHG scatterers. The available optical elements inside the commercial microscope are, in general, not designed for polarization sensitive measurements. Therefore, during the propagation of the excitation light, an ellipticity is introduced and thus, the light arriving at the sample plane is no longer a linearly polarized light. For p-SHG microscopy, excitation of tissue by linearly polarized light is an essential requirement. In this report, we described the development of a portable optical module that can be incorporated in the excitation path of existing commercial microscope to perform excitation polarization measurements. We also described the potential issues responsible for imaging artifacts in p-SHG analysis and provided the relevant solutions in terms of calibrations. Finally, as a proof of concept, for the measurement of χ-parameters, an investigation of heart muscle, ovary tissue and osteoarthritic cartilage was performed.

Paper-2: *Analysis of human knee osteoarthritic cartilage using polarization sensitive second harmonic generation microscopy.*

During the progression of osteoarthritis replacement of extracellular matrix of cartilage takes place. It is reported that the type of cartilage in repaired tissue is not generally hyaline (collagen II) but fibrocartilage (collagen I)[94,95]. Fibrocartilage is not as good as hyaline cartilage in terms of adaptation to mechanical forces. Hence, it is important to differentiate the type of cartilage, a parameter which could be used in assessment of cartilage and may serve as an intrinsic biomarker for the diagnosis of osteoarthritis. In this report, by applying p-SHG imaging technique, we found the presence of fibrocartilage even in early stage (ICRS Grade I) of osteoarthritis that would otherwise only be visible by histology in advanced stage of osteoarthritis. Moreover, we were also able to quantify the alteration in the collagen molecules in terms of the pitch angle of the peptide backbone and of the methylene side chain; features which are well beyond the level of optical resolution.

Paper-3: *Nonlinear optical microscopy of early stage (ICRS Grade-I) osteoarthritic human cartilage.*

In comparison to current clinical imaging modalities (e.g., CT, MRI, Ultrasound), nonlinear optical microscopy (NLOM) may provide improved characterization of articular cartilage that can be used to evaluate cartilage disorders and understand the mechanism behind progression of osteoarthritis. Although, using NLOM a few studies of degenerative cartilage were performed, the investigation of human tissue rather than animal model, especially with early stage of osteoarthritic cartilage, is essential and potentially more relevant to the clinical application. In this investigation, by using nonlinear optical microscopy (NLOM), we have investigated early stage (ICRS Grade-I) osteoarthritic cartilage obtained from the human knee. In this investigation, we observed that within ICRS Grade-I, distinct morphological features were present that may represent different phase of cartilage degradation during progression of OA. SHG microscopy shows microsplits even in early stage of osteoarthritis that would otherwise not be visible in other clinical imaging modalities. Moreover, ripple/wrinkle like feature was also observed in the specimen collected from non-load bearing areas of the knee. Visibility of such novel morphological and structural features in early stage osteoarthritis demonstrate that SHG microscopy may be a promising potential tool that can be used for *in vivo* diagnosis of osteoarthritis.

Paper-4: *Optical investigation of osteoarthritic human cartilage (ICRS Grade) by confocal Raman spectroscopy: A pilot study.*

Currently used clinical imaging modalities (e.g., CT, MRI) provide unique and often complementary information to the rheumatologist. However, these modalities fail to provide crucial information about the biochemical composition of the ECM at the molecular level. Biomolecular changes in the cartilage matrix during the early stage of osteoarthritis may be detected by Raman spectroscopy. Most Raman spectroscopic investigations of osteoarthritis are focused on the analysis of bone. Because the underlying bone is exposed only during the advanced stage of osteoarthritis (i.e., ICRS Grade IV), to detect early-stage osteoarthritis *in vivo*, it is necessary to perform Raman analysis on the articular cartilage rather than on the bone. In this investigation, we have demonstrated the feasibility of Raman spectroscopy for biochemical analysis in different stages of human osteoarthritic cartilage. Relative assessment of proteoglycan and amide content was performed and their respective indication was discussed. We also found that there is high positive correlation between two different clinical grading systems (ICRS Vs. OARSI)[48,96] of osteoarthritis. Our proof of concept investigation encourages the development of a Raman arthroscope for *in vivo* biochemical assessment of cartilage disorder.

Paper-5: *Label free optical detection of ICRS grade in osteoarthritic chondrocytes by Raman microspectroscopy.*

As chondrocytes is the only formative cell type available in hyaline cartilage, the degeneration in articular cartilage and thus, progression of osteoarthritis process can be characterized by changes in these cells[97-99] . Several studies show that OA disease advancement is associated with increased chondrocyte cell death[49]. Investigations at the cellular level are, therefore, important in understanding the progression of musculoskeletal disorders. To our knowledge, we have performed the first Raman analysis of osteoarthritic chondrocytes. In this study, chondrocytes were isolated from osteoarthritic cartilage of ICRS Grade-I, II and III. Grade-IV is not included in the study because it represents exposed bone and almost no cartilage. Our investigation clearly indicates changes in protein vibrations. The magnitude of the area represented by amide-I peak is decreasing consistently with increase in the grade of OA. A similar trend was observed with the peak of amide III and phenylalanine. Another spectral feature associated with cell death (1304 cm^{-1}) was observed to be increasing with progression of OA, which is in agreement with previous studies. Additionally, the principal component analysis indicated that chondrocytes

associated with ICRS grade II and III are more heterogeneous (i.e., cells are in different stages) than ICRS grade-I.

- **Conclusion and future perspective**

OA is the leading cause of permanent work incapacitation and one of the most common reasons for visiting primary care physicians[97]. It is one of the fastest increasing socioeconomic burdens[100]. The understanding of OA at both the basic as well as the clinical level has increased over the past few decades but it seems like a paradox that probably more questions have been raised than answered! In many studies of articular cartilages in OA, wide variations in degenerative changes are observed possibly due to overlapping of multiple disorders which is, in fact, an inherent feature of OA.

Current clinical modalities provide unique and complementary informations relevant for the diagnosis and progression of OA. However, they currently fail to provide the information at high resolution or with chemical specificity. NLOM and Raman spectroscopy are emerging as important techniques with ever increasing numbers of important application in the field of biology, medicine, chemistry and physics. The progression of osteoarthritis (OA) is directly associated with degeneration of the articular cartilage. SHG microscopy is highly specific to collagen fibers which is one of the major constituents of articular cartilage and can provide high resolution images. Therefore, it can perform better structural characterization of articular cartilage compared to other existing clinical modalities, and thus, may provide hidden features that can help in the exploration of underlying mechanism of OA. Additionally, TPEF microscopy can complement SHG microscopy by proving other relevant informations associated with ECM and cells as well.

Our investigation with SHG microscopy has shown several novel features. First, different phases of osteoarthritis were observed within ICRS Grade-I specimens. In initial stage of OA, superficial layer of cartilage was present while during progression of OA, it was eroded or worn out and therefore, only the middle to deep layer of cartilage was visible. In samples with eroded superficial layer, as second feature, microsplits were observed that might appear because of imbalance of shear stresses in knee joint due to the absence of a superficial layer in cartilage structure. Third, wrinkle/ripple like structures were also observed in early stage (ICRS Grade-I) osteoarthritic cartilages which are supposed to a characteristic feature of OA[101-103]. By using p-SHG microscopy, and thus, obtaining χ value parameter, we observed that fibrocartilage (collagen-I) can be differentiated from hyaline cartilage and is observed even in early stage of OA. Fibrocartilage is typically only visible in

histology in advanced stage of OA. We also quantified the change in peptide and methylene pitch angle due to structural modification of collagen fiber. Since limited sample was available in our investigation, large scale investigation is further required to validate these features.

Now, where do we expect the use of NLOM to go from here? We have performed investigation on early stage (ICRS Grade-I) of OA and demonstrated the possibility for finding early stage morphological features in osteoarthritic cartilage using NLOM. All measurements were performed in the backscattered imaging mode. Our findings might be of importance for further *in vivo* assessment of articular cartilage using a miniaturized NLOM probe, which necessarily uses the backscattered signal. As another direction, to understand the mechanism behind the disease progression, the analysis with other ICRS Grades of OA (i.e., Grade II, III and IV) can be performed. Besides investigation of surface morphology, the analysis with different layer of cartilage, after sectioning, may reveal new features. For example, in a cartilage section (ICRS Grade-I) at the depth ~1000 µm from articular surface, TPEF image shows bright peri-cellular feature (figure 9) around the lacuna. This feature might be appeared due to occurrence of collagen VI around the pericellular lacuna[104]. Further detailed investigation is required. Besides investigation of osteoarthritic cartilage (ICRS Grade-I,II,III), the analysis with normal human cartilage may lead towards a diagnosis of OA. Due to ethical reason, the normal human cartilage was not available at the moment.
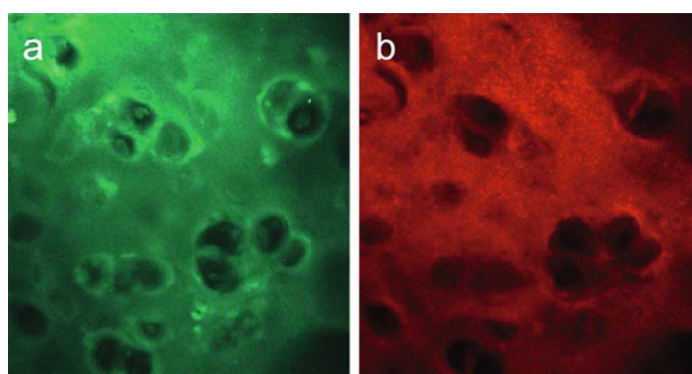

Figure 9: TPEF (a) and corresponding SHG (b) image of an osteoarthritic (ICRS Grade-I) cartilage section at ~1000 µm depth from the articular surface (size: 225 µm × 225 µm). A bright pericellular structure around the lacuna can be seen in TPEF image.

While NLOM can provide highly resolved structural and morphological features, it lacks in providing information about changes in biochemical compositions in articular cartilage. Biochemical changes occur before they appear as a morphological or structural features[63]. Raman spectroscopy can provide such information in intact cartilage without adding any external labels or dyes and any restriction on sample environment.

Previous studies on OA by Raman spectroscopy have primarily focused on bone. The underlying bone is exposed only during the advanced stage of osteoarthritis (i.e., ICRS Grade IV). Our pilot investigation demonstrates that Raman spectroscopy may be used to characterize the human articular cartilage based on biochemical compositions. The optics involved in Raman spectroscopy are compatible with modern clinical arthroscopes. Hence, with the advancement of technology, a miniaturize Raman probe can be integrated with a clinical arthroscope and thus, potentially may lead to *in vivo* Raman arthroscopy that can serve as a tool for early diagnosis. Another direction could be finding other biochemical features which may enhance the proposed method's ability to discern degraded cartilage even at early stage of manifestation. It is proposed that the progression of OA is associated with early loss of bone owing to increased bone remodeling which finally leads to the loss of cartilage[105]. It has been suggested that the remodeling of subchondral bone plays a role in the progression of OA[106]. However, it remains unclear whether bone or cartilage changes occur earlier?[107-109]. The answer remains unclear but may play an important role in understanding the progression of the disease. As a future work, we will attempt to determine whether biochemical Raman analysis of cartilage and associated underlying subchondral bone can answer this question or not. Relevant spectroscopic data have been collected and further investigation is yet to be done.

Raman microspectroscopy provides a noninvasive and nondestructive analytical capability at the scale of single cells in the absence of fluorescent stains. Our study encourages further Raman investigation of chondrocytes. It may provide more information about proliferation/cell death (apoptosis), degradation and phenotypic alteration of the articular chondrocytes. More biochemical informations at the cellular level may clarify osteoarthritic features in a better way[110]. Moreover, live cell analysis may help further in understanding the behavior of osteoarthritic chondrocytes. Such manifold analytical possibilities are simply not found in any other microscopic technique[111]. However, despite a number of publications and a few clinical trials for various biomedical applications[112] (e.g., diagnosis of skin disease, diagnosis of cancer, identification of pathogenic micro-organism etc.), Raman spectroscopy

is still a young discipline. Nevertheless, in the light of diagnosis and treatment of bone and cartilage disease for the use in Orthopaedics, it has huge potential.
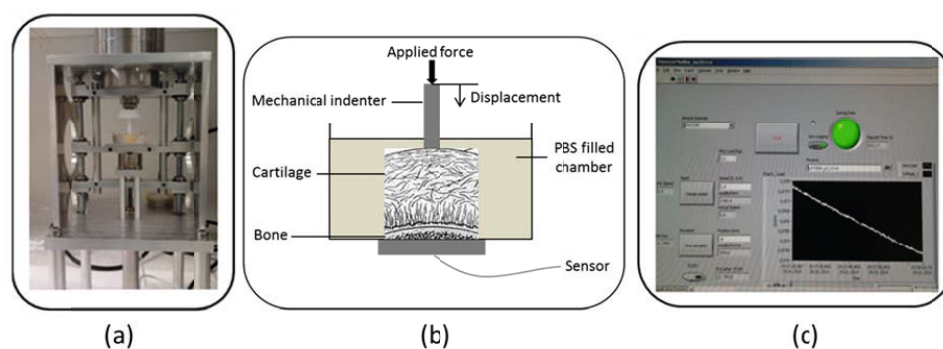
Figure 10: Development of a mechanical indenter for biomechanical characterization of cartilage. (a) A photograph of the device. (b) Schematic diagram (c) Lab-view based software to control the device

Due to the complex nature of OA, it is worth to note that the measurement of the degradation of articular cartilage either by morphology or biochemical compositions may not be sufficient. Functional integrity between structural, biochemical and biomechanical properties of articular cartilage in a joint is essential to maintain the homeostasis (metabolic equilibrium) of chondrocytes. Therefore, it is necessary to consider structural, biochemical and biomechanical features together to evaluate the degradation of articular cartilage. In order to understand the viscoelastic behavior, biomechanical characterization of osteoarthritic cartilage (ICRS Grade-I,II,III) is in progress. We have developed a mechanical indenter in our laboratory (figure 10). Data have been collected and further investigations have to be done in the near future. Moreover, the high resolution SHG images of osteoarthritic cartilage are well-suited for modelling of articular cartilage especially to map into a finite element (FE) mesh in an element-wise sense[113]. Therefore, the data can be sampled at a specified high resolution to determine FE meshes and input suits the specific needs[113]. By utilizing our experimental data as an input for biomechanical modelling, it may enable FE simulations of articular cartilage more close to the real application that may enhance our knowledge further about biomechanical behavior of musculoskeletal tissue in an osteoarthritic joint.

In conclusion, a multimodal minimal invasive, high resolution and label free approach i.e., combined assessment of NLOM microscopy, Raman spectroscopy and mechanical indentation together with clinical imaging and symptoms may provide the most comprehensive assessment of the cartilage disorder, which may eventually lead to the early diagnosis of OA.

There are no pain receptors found in cartilage. Therefore, it is difficult to say that any correlation between pain and morphological/biochemical/biomechanical feature can be found. Nevertheless, detailed knowledge and enhanced understanding will help in early diagnosis that will lead towards right treatment. By the development of new techniques and tools more accurate and objective informations will be valuable academically. However, the clinical value of new tools will be known only after many years of clinical trials.

REFERENCES

1   Merx, H. *et al.* International variation in hip replacement rates. *Annals of the rheumatic diseases* **62**, 222-226 (2003).

2   NIH Consensus Statement on total knee replacement December 8-10, 2003. *The Journal of bone and joint surgery. American volume* **86a**, 1328-1335 (2004).

3   Wieland, H. A., Michaelis, M., Kirschbaum, B. J. & Rudolphi, K. A. Osteoarthritis - an untreatable disease? *Nature reviews. Drug discovery* **4**, 331-344, doi:10.1038/nrd1693 (2005).

4   Hunter, D. J., Schofield, D. & Callander, E. The individual and socioeconomic impact of osteoarthritis. *Nat Rev Rheumatol* **10**, 437-441, doi:10.1038/nrrheum.2014.44 (2014).

5   Kellgren, J. H. & Lawrence, J. S. Radiological assessment of osteo-arthrosis. *Annals of the rheumatic diseases* **16**, 494-502 (1957).

6   Ryu, J. H. *et al.* Measurement of MMP Activity in Synovial Fluid in Cases of Osteoarthritis and Acute Inflammatory Conditions of the Knee Joints Using a Fluorogenic Peptide Probe-Immobilized Diagnostic Kit. *Theranostics* **2**, 198-206, doi:10.7150/thno.3477 (2012).

7   Klaus Kuettner & Goldberg, V. *Osteoarthritic Disorders. Chapter 1: The classification and Diagnosis of Osteoarthritis.*, (American Academy of Orthopaedic Surgeons., 1995).

8   Chang, C. B., Seong, S. C. & Kim, T. K. Evaluations of radiographic joint space – do they adequately predict cartilage conditions in the patellofemoral joint of the patients undergoing total knee arthroplasty for advanced knee osteoarthritis? *Osteoarthritis and Cartilage* **16**, 1160-1166, doi:http://dx.doi.org/10.1016/j.joca.2008.02.012 (2008).

9   Link, T. M. *Cartilage Imaging: Significance, Techniques, and New Developments. Chapter 4.*, Springer (2011).

10   Scott, W. W., Jr. *et al.* Reliability of grading scales for individual radiographic features of osteoarthritis of the knee. The Baltimore longitudinal study of aging atlas of knee osteoarthritis. *Investigative radiology* **28**, 497-501 (1993).

11   Cooper, C. *et al.* Radiographic assessment of the knee joint in osteoarthritis. *Annals of the rheumatic diseases* **51**, 80-82 (1992).

12   Le Graverand, M. P. *et al.* Assessment of the radioanatomic positioning of the osteoarthritic knee in serial radiographs: comparison of three acquisition techniques. *Osteoarthritis and cartilage / OARS, Osteoarthritis Research Society* **14 Suppl A**, 37-43, doi:10.1016/j.joca.2006.02.024 (2006).

13   Conaghan, P. G., Hunter, D. J., Maillefert, J. F., Reichmann, W. M. & Losina, E. Summary and recommendations of the OARSI FDA osteoarthritis Assessment of Structural Change Working Group. *Osteoarthritis and cartilage / OARS, Osteoarthritis Research Society* **19**, 606-610, doi:10.1016/j.joca.2011.02.018 (2011).

14   Reichmann, W. M. *et al.* Responsiveness to change and reliability of measurement of radiographic joint space width in osteoarthritis of the knee: a systematic review. *Osteoarthritis and Cartilage* **19**, 550-556, doi:http://dx.doi.org/10.1016/j.joca.2011.01.023 (2011).

15   Guermazi, A., Roemer, F. W., Burstein, D. & Hayashi, D. Why radiography should no longer be considered a surrogate outcome measure for longitudinal assessment of cartilage in knee osteoarthritis. *Arthritis research & therapy* **13**, 247, doi:10.1186/ar3488 (2011).

16   Roemer, F. W. *et al.* Tibiofemoral joint osteoarthritis: risk factors for MR-depicted fast cartilage loss over a 30-month period in the multicenter osteoarthritis study. *Radiology* **252**, 772-780, doi:10.1148/radiol.2523082197 (2009).

17   Disler, D. G., Recht, M. P. & McCauley, T. R. MR imaging of articular cartilage. *Skeletal radiology* **29**, 367-377 (2000).

18   Hodgson, R. J., O'Connor, P. J. & Grainger, A. J. Tendon and ligament imaging. *The British Journal of Radiology* **85**, 1157-1172, doi:10.1259/bjr/34786470 (2012).

19   Neogi, T. *et al.* Subchondral bone attrition may be a reflection of compartment-specific mechanical load: the MOST Study. *Annals of the rheumatic diseases* **69**, 841-844, doi:10.1136/ard.2009.110114 (2010).

20   Lowitz, T. *et al.* Bone marrow lesions identified by MRI in knee osteoarthritis are associated with locally increased bone mineral density measured by QCT. *Osteoarthritis and Cartilage* **21**, 957-964, doi:http://dx.doi.org/10.1016/j.joca.2013.04.006 (2013).

21   Cicuttini, F., Forbes, A., Asbeutah, A., Morris, K. & Stuckey, S. Comparison and reproducibility of fast and conventional spoiled gradient-echo magnetic resonance sequences in the determination of knee cartilage volume. *Journal of orthopaedic research : official publication of the Orthopaedic Research Society* **18**, 580-584, doi:10.1002/jor.1100180410 (2000).

22   Eckstein, F. *et al.* In vivo reproducibility of three-dimensional cartilage volume and thickness measurements with MR imaging. *AJR. American journal of roentgenology* **170**, 593-597, doi:10.2214/ajr.170.3.9490936 (1998).

23   Regatte, R. R., Akella, S. V., Borthakur, A., Kneeland, J. B. & Reddy, R. In vivo proton MR three-dimensional T1rho mapping of human articular cartilage: initial experience. *Radiology* **229**, 269-274, doi:10.1148/radiol.2291021041 (2003).

24   Mosher, T. J. *et al.* Knee articular cartilage damage in osteoarthritis: analysis of MR image biomarker reproducibility in ACRIN-PA 4001 multicenter trial. *Radiology* **258**, 832-842, doi:10.1148/radiol.10101174 (2011).

25   Wheaton, A. J. *et al.* Correlation of T1rho with fixed charge density in cartilage. *Journal of magnetic resonance imaging : JMRI* **20**, 519-525, doi:10.1002/jmri.20148 (2004).

26   Blumenkrantz, G. & Majumdar, S. Quantitative magnetic resonance imaging of articular cartilage in osteoarthritis. *European cells & materials* **13**, 76-86 (2007).

27   Wheaton, A. J. *et al.* Proteoglycan loss in human knee cartilage: quantitation with sodium MR imaging--feasibility study. *Radiology* **231**, 900-905, doi:10.1148/radiol.2313030521 (2004).

28   Borthakur, A. *et al.* In vivo triple quantum filtered twisted projection sodium MRI of human articular cartilage. *Journal of magnetic resonance (San Diego, Calif. : 1997)* **141**, 286-290, doi:10.1006/jmre.1999.1923 (1999).

29   Reddy, R. *et al.* Sodium MRI of human articular cartilage in vivo. *Magnetic resonance in medicine : official journal of the Society of Magnetic Resonance in Medicine / Society of Magnetic Resonance in Medicine* **39**, 697-701 (1998).

30   Burstein, D., Bashir, A. & Gray, M. L. MRI techniques in early stages of cartilage disease. *Investigative radiology* **35**, 622-638 (2000).

31   McKenzie, C. A., Williams, A., Prasad, P. V. & Burstein, D. Three-dimensional delayed gadolinium-enhanced MRI of cartilage (dGEMRIC) at 1.5T and 3.0T. *Journal of magnetic resonance imaging : JMRI* **24**, 928-933, doi:10.1002/jmri.20689 (2006).

32   Aisen, A. M. *et al.* Sonographic evaluation of the cartilage of the knee. *Radiology* **153**, 781-784, doi:10.1148/radiology.153.3.6387794 (1984).

33   Guermazi, A. *et al.* Osteoarthritis: current role of imaging. *The Medical clinics of North America* **93**, 101-126, xi, doi:10.1016/j.mcna.2008.08.003 (2009).

34   Keen, H. I. & Conaghan, P. G. Ultrasonography in osteoarthritis. *Radiologic clinics of North America* **47**, 581-594, doi:10.1016/j.rcl.2009.04.007 (2009).

35   Haraoui, B., Pelletier, J. P., Cloutier, J. M., Faure, M. P. & Martel-Pelletier, J. Synovial membrane histology and immunopathology in rheumatoid arthritis and osteoarthritis. In vivo effects of antirheumatic drugs. *Arthritis and rheumatism* **34**, 153-163 (1991).

36   Daichi Hayashi, F. W. R. & Mohamed Jarraya, a. A. G. in *Geriatric Imaging*   (ed G. Guglielmi et al.) Ch. 5, (Springer-Verlag Berlin Heidelberg, 2013).

37   Chu, C. R. *et al.* Clinical optical coherence tomography of early articular cartilage degeneration in patients with degenerative meniscal tears. *Arthritis and rheumatism* **62**, 1412-1420, doi:10.1002/art.27378 (2010).

38   Chhablani, J., Krishnan, T., Sethi, V. & Kozak, I. Artifacts in optical coherence tomography. *Saudi Journal of Ophthalmology* **28**, 81-87, doi:http://dx.doi.org/10.1016/j.sjopt.2014.02.010 (2014).

39   Malley, M. J. & Chu, C. R. Arthroscopic Optical Coherence Tomography in Diagnosis of Early Arthritis. *Minimally Invasive Surgery,* article ID 671308, doi:10.1155/2011/671308 (2011).

40   Buckwalter, J. A. & Mankin, H. J. Articular Cartilage. Part I: Tissue Design and Chondrocyte-Matrix Interactions. *The Journal of Bone & Joint Surgery* **79**, 600-611 (1997).

41   Steward, A., Liu, Y. & Wagner, D. Engineering cell attachments to scaffolds in cartilage tissue engineering. *JOM* **63**, 74-82, doi:10.1007/s11837-011-0062-x (2011).

42   Sophia Fox, A. J., Bedi, A. & Rodeo, S. A. The Basic Science of Articular Cartilage: Structure, Composition, and Function. *Sports Health* **1**, 461-468, doi:10.1177/1941738109350438 (2009).

43   Otte, P. [The nature of coxarthrosis and principles of its management]. *Deutsches medizinisches Journal* **20**, 341-346 (1969).

44   Heep, H., Hilken, G., Hofmeister, S. & Wedemeyer, C. Osteoarthitis of leptin-deficient ob/ob mice in response to biomechanical loading in micro-CT. *International journal of biological sciences* **5**, 265-275 (2009).

45   Collins, D.H. The pathology of osteoarthritis. *British journal of rheumatology.* **1**, 248-262 (1939).

46   Collins, D. H. *The Pathology of Articular and Spinal Diseases*. (Edward Arnold & Co. London, pp. 74-115, 1949).

47   Mankin, H. J., Dorfman, H., Lippiello, L. & Zarins, A. Biochemical and metabolic abnormalities in articular cartilage from osteo-arthritic human hips. II. Correlation of morphology with biochemical and metabolic data. *The Journal of bone and joint surgery. American volume* **53**, 523-537 (1971).

48   Pritzker, K. P. *et al.* Osteoarthritis cartilage histopathology: grading and staging. *Osteoarthritis and cartilage / OARS, Osteoarthritis Research Society* **14**, 13-29, doi:10.1016/j.joca.2005.07.014 (2006).

49   Horton, W. E., Jr., Yagi, R., Laverty, D. & Weiner, S. Overview of studies comparing human normal cartilage with minimal and advanced osteoarthritic cartilage. *Clinical and experimental rheumatology* **23**, 103-112 (2005).

50   Horton, W. E., Jr., Bennion, P. & Yang, L. Cellular, molecular, and matrix changes in cartilage during aging and osteoarthritis. *Journal of musculoskeletal & neuronal interactions* **6**, 379-381 (2006).

51   Mandelbaum, B. & Waddell, D. Etiology and pathophysiology of osteoarthritis. *Orthopedics* **28**, s207-214 (2005).

52   Ostergaard, K., Andersen, C. B., Petersen, J., Bendtzen, K. & Salter, D. M. Validity of histopathological grading of articular cartilage from osteoarthritic knee joints. *Annals of the rheumatic diseases* **58**, 208-213 (1999).

53   Ostergaard, K., Petersen, J., Andersen, C. B., Bendtzen, K. & Salter, D. M. Histologic/histochemical grading system for osteoarthritic articular cartilage:

reproducibility and validity. *Arthritis and rheumatism* **40**, 1766-1771, doi:10.1002/1529-0131(199710)40:10<1766::AID-ART7>3.0.CO;2-B (1997).

54 Helmchen, F. & Denk, W. Deep tissue two-photon microscopy. *Nature methods* **2**, 932-940, doi:10.1038/nmeth818 (2005).

55 Zipfel, W. R., Williams, R. M. & Webb, W. W. Nonlinear magic: multiphoton microscopy in the biosciences. *Nature biotechnology* **21**, 1369-1377, doi:10.1038/nbt899 (2003).

56 Campagnola, P. J. *et al.* Three-dimensional high-resolution second-harmonic generation imaging of endogenous structural proteins in biological tissues. *Biophysical journal* **82**, 493-508, doi:10.1016/s0006-3495(02)75414-3 (2002).

57 Schenke-Layland, K. Non-invasive multiphoton imaging of extracellular matrix structures. *Journal of Biophotonics* **1**, 451-462, doi:10.1002/jbio.200810045 (2008).

58 Zipfel, W. R. *et al.* Live tissue intrinsic emission microscopy using multiphoton-excited native fluorescence and second harmonic generation. *Proceedings of the National Academy of Sciences of the United States of America* **100**, 7075-7080, doi:10.1073/pnas.0832308100 (2003).

59 Chen, W. L. *et al.* Second harmonic generation χ tensor microscopy for tissue imaging. *Applied Physics Letters* **94**, doi:http://dx.doi.org/10.1063/1.3132062 (2009).

60 Kumar, R. *et al.* Polarization second harmonic generation microscopy provides quantitative enhanced molecular specificity for tissue diagnostics. *Journal of Biophotonics, early view available online,* doi:10.1002/jbio.201400086 (2014).

61 Bao, H. & Gu, M. A 0.4-mm-diameter probe for nonlinear optical imaging. *Optics express* **17**, 10098-10104 (2009).

62 Tang, S. *et al.* Design and implementation of fiber-based multiphoton endoscopy with microelectromechanical systems scanning. *Journal of biomedical optics* **14**, 034005, doi:10.1117/1.3127203 (2009).

63 Morris, D. M. & Roessler, B. J. Future spectroscopic diagnostics in osteoarthritis. *Future Rheumatol.* **1**, 383-386 (2006).

64 Karen, A. E. Raman spectroscopy detection of molecular changes associated with osteoarthritis. *PhD Thesis, University of Michigan.* (2009).

65 John R. Ferraro, K. N., Chris W. Brown. *Introductory Raman Spectroscopy*. (Academic Press, 2002).

66   Chan, J., Fore, S., Wachsmann-Hogiu, S. & Huser, T. Raman spectroscopy and microscopy of individual cells and cellular components. *Laser & Photonics Reviews* **2**, 325-349, doi:10.1002/lpor.200810012 (2008).

67   Nyman, J. S. *et al.* Measuring differences in compositional properties of bone tissue by confocal Raman spectroscopy. *Calcified tissue international* **89**, 111-122, doi:10.1007/s00223-011-9497-x (2011).

68   Dehring, K. A. *et al.* Identifying chemical changes in subchondral bone taken from murine knee joints using Raman spectroscopy. *Applied spectroscopy* **60**, 1134-1141, doi:10.1366/000370206778664743 (2006).

69   Kerns, J. G. *et al.* Raman spectroscopy reveals evidence for early bone changes in Osteoarthritis. *Bone & Joint Journal Orthopaedic Proceedings Supplement* **95B**, 45 (2013).

70   Khan., A. F. *et al.* Raman Spectroscopy of Natural Bone and Synthetic Apatites. *Applied Spectroscopy Reviews.* **48**, 329-355, doi:10.1080/05704928.2012.721107 (2013).

71   Buchwald, T. *et al.* Identifying compositional and structural changes in spongy and subchondral bone from the hip joints of patients with osteoarthritis using Raman spectroscopy. *Journal of biomedical optics* **17**, 017007, doi:10.1117/1.JBO.17.1.017007 (2012).

72   Morris, M. D. & Mandair, G. S. Raman assessment of bone quality. *Clinical orthopaedics and related research* **469**, 2160-2169, doi:10.1007/s11999-010-1692-y (2011).

73   Bonifacio, A. *et al.* Chemical imaging of articular cartilage sections with Raman mapping, employing uni- and multi-variate methods for data analysis. *The Analyst* **135**, 3193-3204, doi:10.1039/c0an00459f (2010).

74   Lim, N. S., Hamed, Z., Yeow, C. H., Chan, C. & Huang, Z. Early detection of biomolecular changes in disrupted porcine cartilage using polarized Raman spectroscopy. *Journal of biomedical optics* **16**, 017003, doi:10.1117/1.3528006 (2011).

75   Pudlas, M., Brauchle, E., Klein, T. J., Hutmacher, D. W. & Schenke-Layland, K. Non-invasive identification of proteoglycans and chondrocyte differentiation state by Raman microspectroscopy. *Journal of Biophotonics* **6**, 205-211, doi:10.1002/jbio.201200064 (2013).

76   Buck, R. J., Wirth, W., Dreher, D., Nevitt, M. & Eckstein, F. Frequency and spatial distribution of cartilage thickness change in knee osteoarthritis and its relation to

clinical and radiographic covariates - data from the osteoarthritis initiative. *Osteoarthritis and cartilage / OARS, Osteoarthritis Research Society* **21**, 102-109, doi:10.1016/j.joca.2012.10.010 (2013).

77   Jess, P. R. *et al.* Early detection of cervical neoplasia by Raman spectroscopy. *International journal of cancer. Journal international du cancer* **121**, 2723-2728, doi:10.1002/ijc.23046 (2007).

78   Kast, R. E. *et al.* Raman spectroscopy can differentiate malignant tumors from normal breast tissue and detect early neoplastic changes in a mouse model. *Biopolymers* **89**, 235-241, doi:10.1002/bip.20899 (2008).

79   Crow, P. *et al.* The use of Raman spectroscopy to identify and grade prostatic adenocarcinoma in vitro. *British journal of cancer* **89**, 106-108, doi:10.1038/sj.bjc.6601059 (2003).

80   Klein, K. *et al.* Label-free live-cell imaging with confocal Raman microscopy. *Biophysical journal* **102**, 360-368, doi:10.1016/j.bpj.2011.12.027 (2012).

81   Franken, P., Hill, A., Peters, C. & Weinreich, G. Generation of Optical Harmonics. *Physical Review Letters* **7**, 118-119 (1961).

82   Seka, W., Jacobs, S. D., Rizzo, J. E., Boni, R. & Craxton, R. S. Demonstration of high efficiency third harmonic conversion of high power Nd-glass laser radiation. *Optics Communications* **34**, 469-473, doi:http://dx.doi.org/10.1016/0030-4018(80)90419-8 (1980).

83   Su, P. J., Chen, W. L., Chen, Y. F. & Dong, C. Y. Determination of Collagen Nanostructure from Second-Order Susceptibility Tensor Analysis. *Biophysical journal* **100**, 2053-2062, doi:10.1016/j.bpj.2011.02.015 (2011).

84   Su, P. J. *et al.* The discrimination of type I and type II collagen and the label-free imaging of engineered cartilage tissue. *Biomaterials* **31**, 9415-9421, doi:http://dx.doi.org/10.1016/j.biomaterials.2010.08.055 (2010).

85   Barry R. Masters and Peter So, E. *Handbook of Biomedical Nonlinear Optical Microscopy*. (Oxford University Press, 2008).

86   New, G. *Introduction to Nonlinear Optics*. (Cambridge University Press, 2011).

87   LaComb, R., Nadiarnykh, O., Townsend, S. S. & Campagnola, P. J. Phase matching considerations in second harmonic generation from tissues: Effects on emission directionality, conversion efficiency and observed morphology. *Optics Communications* **281**, 1823-1832, doi:http://dx.doi.org/10.1016/j.optcom.2007.10.040 (2008).

88   Göppert-Mayer, M. Über Elementarakte mit zwei Quantensprüngen. *Annalen der Physik* **401**, 273-294, doi:10.1002/andp.19314010303 (1931).

89   Kaiser, W. and Garrett, C. Two-Photon Excitation in CaF_2: Eu^{2+}. *Physical Review Letters* **7**, 229-231 (1961).

90   Sheppard, C. and Gu, M. Image formation in two-photon fluorescence microscopy. *Optik* **86**, 104-106 (1990).

91   Gu, M. & Sheppard, C. J. R. Comparison of three-dimensional imaging properties between two-photon and single-photon fluorescence microscopy. *Journal of Microscopy* **177**, 128-137, doi:10.1111/j.1365-2818.1995.tb03543.x (1995).

92   So, P. T., Dong, C. Y., Masters, B. R. & Berland, K. M. Two-photon excitation fluorescence microscopy. *Annual review of biomedical engineering* **2**, 399-429, doi:10.1146/annurev.bioeng.2.1.399 (2000).

93   Hell, S. W. *et al.* Two-photon near- and far-field fluorescence microscopy with continuous-wave excitation. *Opt. Lett.* **23**, 1238-1240, doi:10.1364/OL.23.001238 (1998).

94   Yeh, A. T. *et al.* Nonlinear optical microscopy of articular cartilage. *Osteoarthritis and cartilage / OARS, Osteoarthritis Research Society* **13**, 345-352, doi:10.1016/j.joca.2004.12.007 (2005).

95   Falah, M., Nierenberg, G., Soudry, M., Hayden, M. & Volpin, G. Treatment of articular cartilage lesions of the knee. *International Orthopaedics (SICOT)* **34**, 621-630, doi:10.1007/s00264-010-0959-y (2010).

96   Brittberg, M.; glietti, P.; Gambardella, R.; Hangody, L.; Hauselmann, H.J.; Jakob, R.P.; Levine, D.; Lohmander, S.; Mandelbaum, B.R.; Peterson, L.; et al. ICRS Cartilage Injury Evaluation Package. In Proceedings of the 3rd ICRS Meeting, Göteborg, Sweden, 28 April 2000. Available online: http://www.cartilage.org/_files/contentmanagement/ICRS_evaluation.pdf

97   Blanco, F. J., Rego, I. & Ruiz-Romero, C. The role of mitochondria in osteoarthritis. *Nat Rev Rheumatol* **7**, 161-169, doi:10.1038/nrrheum.2010.213 (2011).

98   van der Kraan, P. M. & van den Berg, W. B. Chondrocyte hypertrophy and osteoarthritis: role in initiation and progression of cartilage degeneration? *Osteoarthritis and Cartilage* **20**, 223-232, doi:http://dx.doi.org/10.1016/j.joca.2011.12.003 (2012).

99   Price, J. S. *et al.* The role of chondrocyte senescence in osteoarthritis. *Aging Cell* **1**, 57-65, doi:10.1046/j.1474-9728.2002.00008.x (2002).

100   Hunter, D. J., Schofield, D. & Callander, E. The individual and socioeconomic impact of osteoarthritis. *Nat Rev Rheumatol* **10**, 437-441, doi:10.1038/nrrheum.2014.44 (2014).

101   Mansfield, J. C., Winlove, C. P., Moger, J. & Matcher, S. J. Collagen fiber arrangement in normal and diseased cartilage studied by polarization sensitive nonlinear microscopy. *Journal of biomedical optics* **13**, 044020, doi:10.1117/1.2950318 (2008).

102   David, G. and Murray, M. D. Experimentally Induced Arthritis Using Intra-articular Papain. *Arthritis & Rheumatism* **7**, 211-219 (1964).

103   Saïed, A. *et al.* Assessment of Articular Cartilage and Subchondral Bone: Subtle and Progressive Changes in Experimental Osteoarthritis Using 50 MHz Echography In Vitro. *Journal of Bone and Mineral Research* **12**, 1378-1386, doi:10.1359/jbmr.1997.12.9.1378 (1997).

104   Werkmeister, E. *et al.* 381 Second harmonic generation imaging and collageneous matrix modification in osteoarthritis disease. *Osteoarthritis and Cartilage* **16**, S164, doi:10.1016/S1063-4584(08)60422-7.

105   Burr, D. B. & Gallant, M. A. Bone remodelling in osteoarthritis. *Nat Rev Rheumatol* **8**, 665-673, doi:10.1038/nrrheum.2012.130 (2012).

106   Hayami, T. *et al.* The role of subchondral bone remodeling in osteoarthritis: reduction of cartilage degeneration and prevention of osteophyte formation by alendronate in the rat anterior cruciate ligament transection model. *Arthritis and rheumatism* **50**, 1193-1206, doi:10.1002/art.20124 (2004).

107   Burr, D. B. The importance of subchondral bone in osteoarthrosis. *Current opinion in rheumatology* **10**, 256-262 (1998).

108   Bailey, A. J. & Mansell, J. P. Do subchondral bone changes exacerbate or precede articular cartilage destruction in osteoarthritis of the elderly? *Gerontology* **43**, 296-304 (1997).

109   Sharma, A., Jagga, S., Lee, S.-S. & Nam, J.-S. Interplay between Cartilage and Subchondral Bone Contributing to Pathogenesis of Osteoarthritis. *International Journal of Molecular Sciences* **14**, 19805-19830 (2013).

110   Sandell, L. J. & Aigner, T. Articular cartilage and changes in arthritis. An introduction: cell biology of osteoarthritis. *Arthritis research* **3**, 107-113 (2001).

111   Schie, I. W. & Huser, T. Methods and applications of Raman microspectroscopy to single-cell analysis. *Applied spectroscopy* **67**, 813-828, doi:10.1366/12-06971 (2013).

112 Choo-Smith, L. P. *et al.* Medical applications of Raman spectroscopy: from proof of principle to clinical implementation. *Biopolymers* **67**, 1-9, doi:10.1002/bip.10064 (2002).

113 Lilledahl, M. B., Pierce, D. M., Ricken, T., Holzapfel, G. A. & Davies Cde, L. Structural analysis of articular cartilage using multiphoton microscopy: input for biomechanical modeling. *IEEE transactions on medical imaging* **30**, 1635-1648, doi:10.1109/tmi.2011.2139222 (2011).

Paper I

Paper II

Content is not included

Paper III

Content is removed due to copyright policy

Paper IV

Paper V

Content is not included